Robust global ocean cooling trend for the pre-industrial Common Era

Helen V. McGregor[1]*, Michael N. Evans[2], Hugues Goosse[3], Guillaume Leduc[4], Belen Martrat[5,6], Jason A. Addison[7], P. Graham Mortyn[8], Delia W. Oppo[9], Marit-Solveig Seidenkrantz[10], Marie-Alexandrine Sicre[11], Steven J. Phipps[12,13], Kandasamy Selvaraj[14], Kaustubh Thirumalai[15], Helena L. Filipsson[16], and Vasile Ersek[17]

[1]School of Earth and Environmental Sciences, Northfields Ave, University of Wollongong, NSW 2522, Australia

[2]Department of Geology and Earth System Science Interdisciplinary Center, University of Maryland, College Park, MD USA

[3]Earth and Life Institute, Université de Louvain, Place pasteur 3, 1348 Louvain-la-Neuve, Belgium

[4]Aix Marseille Université, CNRS, IRD, CEREGE UM34, 13545 Aix-en-Provence Cedex 4, France

[5]Department of Environmental Chemistry, Institute of Environmental Assessment and Water Research (IDÆA), Spanish Council for Scientific Research (CSIC), 08034 Barcelona, Spain

[6]University of Cambridge, Department of Earth Sciences, Downing Street, Cambridge CB2 3EQ, UK

[7]U.S. Geological Survey, 345 Middlefield Rd., MS 910, Menlo Park, CA 94025, USA

[8]Universitat Autonoma de Barcelona, Institute of Environmental Science and Technology (ICTA) and Department of Geography, Bellaterra, Spain

[9]Department of Geology and Geophysics, Woods Hole Oceanographic Institution, Woods Hole, MA 02543

[10]Centre for Past Climate Studies and Arctic Research Centre, Department of Geoscience, Aarhus University, Hoegh-Guldbergs Gade 2, DK-8000 Aarhus C, Denmark

[11]Sorbonne Universités (UPMC, Univ Paris 06)-CNRS-IRD-MNHN, LOCEAN Laboratory, 4 place Jussieu, F-75005 Paris, France

[12]ARC Centre of Excellence for Climate System Science, University of New South Wales, Sydney NSW 2052, Australia

[13]Climate Change Research Centre, University of New South Wales, Sydney NSW 2052, Australia

[14]State Key Laboratory of Marine Environmental Science, Xiamen University, Xiamen 361102, China

[15]Institute for Geophysics, Jackson School of Geosciences, University of Texas at Austin, J. J. Pickle Research Campus, Building 196, 10100 Burnet Road (R2200), Austin, Texas 78758-4445, USA

[16]Department of Geology, Lund University, Sölvegatan 12, SE-223 62 Lund, Sweden

[17]Department of Geography, Northumbria University, Newcastle upon Tyne, NE1 8ST, UK

*Corresponding author: H. V. McGregor, H. V. McGregor, School of Earth and Environmental Sciences, University of Wollongong, Northfields Ave, NSW 2522, Australia. Email: mcgregor@uow.edu.au Telephone: +61 432 897 139

Keywords: sea surface temperature (SST), global ocean, paleoclimate reconstructions, climate model simulations, climate forcing, Common Era

The oceans mediate the response of global climate to natural and anthropogenic forcing. Yet for the past 2000 years, a key interval for understanding the climate response to these forcings, global sea surface temperature changes and the underlying driving mechanisms are poorly constrained. Here we present a global synthesis of sea surface temperatures for the Common Era (CE) derived from 57 individual marine records that meet strict quality control criteria. We observe a cooling trend from 1 to 1800 CE that is robust against explicit tests for potential biases in the reconstructions. Between 801 and 1800 CE the surface cooling trend is qualitatively consistent with an independent synthesis of terrestrial temperature reconstructions, and with sea surface temperature simulated by an ensemble of climate model simulations using best estimates of past external radiative forcings. Single and cumulative forcing climate simulations suggest that the ocean surface cooling trend from 801-1800 CE is not primarily a response to orbital forcing but arises from high frequency of explosive volcanism. The results show that repeated clusters of volcanic eruptions can induce a net negative radiative forcing that results in a centennial and global-scale cooling trend via a decline in mixed-layer oceanic heat content.

Knowledge of natural climate variability is essential to better constrain the uncertainties in projections of 21st century climate change[1-5]. The past 2000 years (2ky) have emerged as a critical interval in this endeavor, with sufficient length to characterize natural decadal-to-centennial scale change, with known external climate forcings[6], and with distinctive patterns of spatio-temporal temperature variations[7]. However, global reconstructions for the full 2ky interval are not available for the ocean, a primary heat reservoir[8] and important regulator of global climate on longer time scales[9-11]. Here we present a global ocean SST synthesis

spanning the Common Era, which shows a cooling trend, which is similar, within uncertainty, to that simulated by realistically-forced climate models for the past millennium. We use the simulations to identify the climate forcing(s) consistent with reconstructed SST variations during the past millennium.

The Ocean2k SST synthesis dataset

Our global synthesis (hereafter the Ocean2k SST synthesis) is based on 57 marine-origin, peer-reviewed, and publicly available SST reconstructions spanning some or all of the past 2ky (Fig. 1; Methods; Supplementary Section 1; Supplementary Table S1; Supplementary Fig. S1). The temporal diversity and spatial distribution of the 57 reconstructions present methodological challenges for generating a global synthesis product:

1. To avoid biases towards reconstructions with greater temporal resolution each SST reconstruction was averaged into 200-year 'bins' (i.e. 200-year averages for 1–200 CE, etc. up to 1801–2000 CE; Methods; Supplementary Section 3). This allows for typical errors on reservoir corrected radiocarbon dates, the most common dating method used for the 57 reconstructions. In addition, the oceans' large thermal inertia and integration of short-term climate variations[10] suggests that at 200-year resolution we may expect a global SST signature to emerge from the data composite.

2. Our network includes near-polar to tropical regions (Fig. 1) that record a wide range of SST means and variances (Supplementary Fig. S1). Consequently, our 200-year binned reconstructions are standardized (Methods) prior to compositing. Standardizing is routinely employed to composite reconstructions with different regional variability[12,13], and (i) minimizes bias due to any individual reconstruction overprinting the average trend[14-16], (ii)

maximizes our chances of extracting a global signal, and (iii) allows us to compare results across regions and climate zones, and against terrestrial and model composites. We also scaled the Ocean2k SST synthesis standardized values back to Celsius temperature units, and find consistent results (Supplementary Section 4).

3. We test the possibility that the Ocean2k SST synthesis includes a spatial bias due to the network's sparse and heterogeneous global distribution. We use six PMIP3-compliant climate model simulations available for the past millennium[4] (Methods; Supplementary Table S4; Supplementary Section 5) and calculate the median correlation field of each model grid point with its model global mean SST for the interval 801–1800 CE. High correlations are found for most locations across the globe (Fig. 1), which suggests that the Ocean2k SST network, on bicentennial time scales, should contain a common global signal.

4. The 57 Ocean2k SST reconstructions are skewed towards ocean basin margins (Fig. 1), where sedimentation rates are sufficiently high to provide centennial scale resolution, which could mean that these locations reflect terrestrial rather than marine climate. However, at 200-year resolution, model-simulated true global temperatures are similar to simulated area-weighted or unweighted composites based on our 57 reconstruction locations (Supplementary Fig. S7). As such, we interpret the Ocean2k SST data synthesis as representative of global SST variations.

Robust long-term cooling trend

The global Ocean2k SST synthesis shows a statistically significant median cooling trend of −0.65 standard deviation units per 1000 years (s.d. units/ky) for the past 2ky, and the cooling

trend is steepest for the 1000–1800 CE interval (Fig. 2a). A SST synthesis weighted by ocean basin area gives similar results (Fig. 2a; Supplementary Section 5). However, the marine climate reconstructions that underpin our synthesis have potential biases related to reconstruction type, signal seasonality, sample resolution, age constraints, location, age model and specific proxy-related issues (Supplementary Table S1; Supplementary Section 6); the Ocean2k SST synthesis could reflect a dominance of some of these biases rather than a global signal.

We investigate the Ocean2k synthesis dataset for these sources of bias via a series of sensitivity tests (Fig. 2b). Here, we divide the Ocean2k reconstructions into sub-populations (Methods), and assess their long-term trends relative to the Ocean2k SST synthesis. The sensitivity tests indicate that the Ocean2k global SST cooling trend is not sensitive to the number of dated levels down-core, sedimentation rates (growth rate for the coral reconstruction), SST reconstruction type (e.g. alkenone etc.), recording season for the reconstruction (seasonality), sampling resolution, or water depth at the coring site (as a measure of coastal proximity; Supplementary Section 6; Fig. 2b). Furthermore, the cooling trend is observed in most ocean basins, across hemispheres, in tropical and extratropical latitudes, and in localities characterized as either upwelling or non-upwelling regions (Fig. 2b). We conclude that the cooling trend observed in the Ocean2k SST synthesis is robust despite these uncertainties.

Centennial scale SST variability

The rate of SST cooling recorded by the Ocean2k SST synthesis for the past 2ky is variable, as observed in the rate of change from each 200-year bin to the next 200-year bin (Fig. 2a;

Supplementary Section 7). Analysis of these bin-to-bin SST changes indicates a statistically significant cooling in all bin-to-bin transitions for the 1001–1800 CE period. In contrast, for the transition to the 1801–2000 CE bin, the most recent 200-year interval, there is instead a statistically significant warming trend of +0.08 s.d. units/100yrs (see Supplementary Table S13 for full test statistics). There is no obvious global-scale Medieval Climate Anomaly (MCA)[2,17], although alternate choices for the centers of each bin might allow for better definition of the MCA interval (Supplementary Fig. S5).

Bin-to-bin cooling is especially pronounced for the transition into the 1201-1400 CE and 1401–1600 CE bins (−0.17 and −0.18 s.d. units/100yrs, respectively; Supplementary Table S13), and the overall coldest 200-year bins are the 1401–1600 CE and 1601–1800 CE bins (−0.70 and −0.71 s.d. units, respectively; Supplementary Table S13). These coldest bin transitions and individual bins are contemporaneous with the onset of the globally-coherent 'Little Ice Age' (LIA) recorded in many Northern and Southern Hemisphere continental regions[7,17,18], suggesting that there was a global ocean SST fingerprint associated with the LIA.

The 1801–2000 CE bin, which includes the post-industrial era, has the widest range of values compared to all other bins (Fig. 2a). We further investigate this result using a subset of 21 SST reconstructions with high precision ages based on ^{210}Pb dating, layer counting, or coral band counting (Supplementary Table S1; Supplementary Figure S10; Supplementary Section 8), which have approximately decadal or better sampling resolution, and which span the 19th and 20th centuries. Although assessment of significance is limited by the number and resolution of the reconstructions, and by the small amount of overlap with historical SST estimates, we find that the composite of reconstructions from tropical and/or *a priori*-defined

non-upwelling regions (see Supplementary Section 1 for definition) are correlated with historical SST warming at the same locations[19] (Supplementary Fig. S10). Further confirmation and analysis of results for the 19th and 20th centuries requires extended historical reanalyses[9,20], higher spatio-temporal resolution SST reconstructions from other marine paleoclimate marine archives[21-23], and climate model simulations[10].

Comparisons with terrestrial paleoclimate data and model simulations

The long-term cooling trend captured by the Ocean2k SST synthesis appears consistent with a similar cooling trend observed in global temperature syntheses that include both marine and terrestrial input reconstructions[2,5,24]. To compare global surface ocean and global land temperature trends, we reconstructed a terrestrial composite of non-marine reconstructions[7,25] (Supplementary Section 9; hereafter the Terrestrial 2k composite), ensuring that independent datasets are used to determine marine and terrestrial signals. The Terrestrial 2k composite shows a cooling trend qualitatively similar to the Ocean2k SST synthesis over the 801–1800 CE interval, the interval with the highest availability of SST reconstruction data and model simulations (Fig. 3; Supplementary Table S14). The probability that either the Ocean2k synthesis or the Terrestrial 2k composite indicates a cooling trend for the 801–1800 CE interval is 82% and 73%, respectively (Methods; Supplementary Table S14). Although some of this agreement presumably arises from the proximity of the marine margins to land, the consistency of the Ocean2k SST synthesis and the Terrestrial 2k composite trends is likely due to a relatively coherent response to a common forcing on bicentennial time scales.

We also composite SST from six PMIP3-compliant simulations driven with realistic natural and anthropogenic forcings, matched to the same locations, time intervals, and seasonality as

the 57 Ocean2k reconstructions (multi-model composite; Fig. 3; Methods). The multi-model composite is also qualitatively consistent with the Ocean2k SST synthesis, and has a more likely (94%) probability of a cooling trend, albeit defined by a pronounced cold 1300 CE bin compared to the Ocean2k SST synthesis. The qualitatively similar cooling trends in the Ocean2k SST synthesis and the multi-model composite are not an artifact of the standardization method (see Supplementary Section 4), and suggest that we may analyze the simulations to infer the mechanisms most likely to explain the paleoclimate data.

External forcing of the global SST cooling

We isolate the forcing, or combination of forcings, that is most qualitatively consistent with the Ocean2k SST cooling trend observed for the past 1000 years (the interval of common overlap) using two models from our multi-model composite (Fig. 4): SST simulated by the CSIRO Mk3L model[26], run with the cumulative addition of orbital (O), greenhouse gas (G), solar (S), and volcanic (V) forcings; and by the LOVECLIM model[27], run with individual forcings as for CSIRO Mk3L, plus land use forcing (L) and with all forcings (All). These simulations were matched to the 57 Ocean2k reconstructions (Methods). The CSIRO Mk3L simulations[26] suggest that OGS forcings combined give rise to only a weak and non-significant cooling trend, and are insufficient to explain the long-term Ocean2k global SST cooling trend (Fig. 4a; Supplementary Table S14). The LOVECLIM simulations[27], run individually with O, G, or S forcings, consistently show that these forcings do not explain the Ocean2k SST cooling trend (Fig. 4b; Supplementary Table S14).

The modest effect of greenhouse gases in generating a global ocean surface cooling trend in the model simulations is likely because greenhouse gas forcing is small prior to 1800 CE

(Supplementary Fig. S4). Similarly, the magnitude of solar forcing, although uncertain[6,28,29], is small, and does not generate a significant cooling trend within the model simulations. However, our analysis cannot rule out regional and global mechanisms in which solar activity force climate change on decadal to centennial time scales[30,31].

The single and cumulatively forced model simulations suggest that orbital forcing has only a minor role in generating a global SST cooling trend for the 801–1800 CE interval. Orbital forcing is associated with changes in insolation that are strongly dependent on the season and the latitude[32], and over the Pleistocene orbital changes forced global climate through amplification mechanisms at high northern latitudes including the well-known ice-albedo amplification[33]. High northern latitude temperature trends during the past millennium[27,34,35] were also attributed to orbital forcing, specifically to declining high northern latitude summer insolation, amplified by feedbacks in the Arctic region and resulting in cooling[34,35]. However, when integrated over the full calendar year and spatially across the globe, the 1–2000 CE change in orbital radiative forcing at the top of the atmosphere is only $+4.4 \times 10^{-3}$ W/m^2 (Ref. 34). Consequently, the CSIRO Mk3L and LOVECLIM models both give weak and non-significant global ocean SST trends for the orbital forcing simulations because the global ocean integrates the average global orbital forcing.

We find that volcanic forcing in CSIRO Mk3L, and volcanic and land use forcings in LOVECLIM, produce a cooling trend most consistent with the Ocean2k SST synthesis (Fig. 4). The role of land use change in forcing the Ocean2k SST cooling trend in the LOVECLIM simulation (Fig. 4b) arises from the increase in surface albedo due to deforestation, inducing a net negative radiative forcing on land. The associated cooling is only partly compensated for by the reduced latent heat flux from lower summer evapotranspiration, resulting in overall

cooling on land that is transmitted globally by the atmospheric circulation[27,36,37]. However, there are large uncertainties in our understanding of land use forcing back in time, and with the simulated effects of land use change on radiative forcing and the hydrological cycle[36,38,39].

Volcanic forcing

The influence of volcanic forcing in driving the SST cooling trend for the past millennium is surprising, since this forcing, although large, is relatively episodic[40,41]. The dominance of volcanic forcing over the 801–1800 CE interval may arise from increased volcanic event frequency and the occurrence of very large events early in the past millennium, and/or internal amplification of volcanic forcing within the climate system[6,42-44] (Supplementary Fig. S4). In particular, large volcanic eruptions between 1150 CE and 1300 CE, and again during the early 15th century, may be responsible for the observed cooling[43,45].

We use an Energy Balance Model[46] (EBM; Supplementary Section 10) to simulate the thermodynamic response of a mixed layer ocean to the volcanic radiative forcing (Fig. 4). The EBM results do not fully match the bin-to-bin changes in the Ocean2k SST synthesis, likely because internal variability is absent in the EBM, there are contributions from other forcings, and because the EBM has a weak long-term memory (the EBM contains no deep-ocean coupling). However, we find that the radiative change from repeated clustering of volcanic eruptions over the past millennium by itself is sufficient to explain a long term cooling trend. This suggests that the Ocean2k SST cooling trend at least for >200-year time scales, might simply represent a first-order thermodynamic response to stochastic volcanic forcing that increased in frequency from the early to late last millennium. A comparison of Northern

Hemisphere reconstructed temperatures with a volcanically-forced upwelling/diffusion EBM reached a similar conclusion[47].

Nonetheless, several dynamical mechanisms have been proposed to explain an amplified ocean response to the volcanic forcing during the past millennium[43,48,49]. Specifically, at decadal time scales the volcanic eruptions could have induced a fast cooling in the tropics, leading to anomalously high pressure over the continents that reduced Atlantic Ocean trade wind stress curl anomalies[49]. The subsequent ocean adjustment propagated the cooling to the high latitudes, and over time, weakened the AMOC, resulting in sea-ice expansion. On centennial time scales, eruptions are thought to have reduced downwelling shortwave radiation, increased surface albedo and led to lower-elevation snowlines in regions north of 60°N (Refs. 43, 48). The associated cooling and increase in sea ice extent further amplified Arctic and North Atlantic cooling[43,48]. Open ocean convection may have declined, weakening the Atlantic Meridional Overturning Circulation (AMOC) and its associated ocean heat transport to the high latitude North Atlantic. In turn, the reduced AMOC may have reduced sea-ice melt, permitting sea ice to persist for a century, thus perpetuating the initial cooling induced by the frequent eruptions in the late 13th century[43,48]. These model results suggest that dynamical mechanisms might transform increases in frequency of volcanic eruptions into a longer term cooling.

We test for changes in AMOC in both the volcanic-only forcing LOVECLIM simulation and in the orbital-greenhouse gas-solar-volcanic forcing CSIRO Mk3L simulation (Supplementary Section 10). We find no persistent weakening of the AMOC in response to the volcanic forcing for the past millennium in either simulation (Supplementary Figs. S12 and S13). Furthermore, while Northern Hemisphere sea ice expands following the late 13th

century volcanic cluster, the increase is transient and likely represents a short-term thermodynamic response, rather than a dynamical feedback. Although these results may be model dependent, they are consistent with analysis of a wider range of models[50]. Taken together, our analysis of EBM and coupled model simulations suggests that at >200-year time scales ocean dynamics may not be required to translate volcanic forcing into a long term cooling trend.

Our Ocean2k SST synthesis, built on rigorous quality control of well-dated SST reconstructions, defines a statistically-significant global SST cooling trend for the pre-industrial Common Era. State-of-the-art climate model simulations using realistic forcing show a qualitatively similar cooling trend. Furthermore, a suite of transient model simulations using single and cumulative forcings suggests that the cooling trend does not arise from orbital or solar forcings, but from the increased frequency and magnitude of explosive volcanism, and with land use forcing also a factor. Our results point to a dominant role for volcanic forcing in driving the global SST cooling trend for the pre-industrial Common Era, with the ocean's thermal response integrating the forcing on these longer time scales. Further improved observational coverage, estimates of radiative forcings, and comparisons with simulations will permit more fine-grained assessments of the mechanisms underlying observed climate change -- past and future.

Methods

The Ocean2k SST synthesis is based on 57 peer-reviewed, publicly-available reconstructions solely from marine archives (Fig. 1; Supplementary Table S1), and listed in the PAGES Ocean2k metadatabase (http://www.pages.unibe.ch/workinggroups/ocean2k/data). Reconstructions are 1) expected to record SST, and 2) have a chronology anchored by at least two ages, within error, between 200 years before the CE (BCE) and present. Only data between the oldest and youngest dates were used (Supplementary Section 1 for additional details). Ages were converted to the CE/BCE time scale and SST calibrations from the original publications are used.

Climate model simulations available from 850 CE were selected from BCC-CSM1-1, CCSM4, FGOALS-s2, LOVECLIM, and MPI-ESM, and available from 801 CE for CSIRO Mk3L. The model forcings follow the Coupled Model Intercomparison Project phase 5/ Paleoclimate Model Intercomparison Project phase 3 (CMIP5/PMIP3) protocol[6]. For this subset of simulations there is no significant drift due to experimental design[24]. Model output was truncated at 1800 CE to focus on the pre-industrial past millennium. For Figure 4, additional LOVECLIM and CSIRO Mk3L simulations were used, driven by selected forcings only (Supplementary Section 2; Supplementary Table S4; Supplementary Fig. S11). EBM details are in Supplementary Section 10. Figures 3 and 4 model simulation time series are from the same location (or if a margin site the nearest straight-line distance grid box), time interval, and season as the 57 SST reconstructions in the Ocean2k synthesis. See Supplementary Section 5 for details on Figure 1 construction.

Binning and Standardization: Data from each of the 57 reconstructions were averaged into 200-year bins, to give 10 bins, centered on 100, 300 CE etc. up to 1900 CE. Each 'binned'

series was then standardized by its average and standard deviation. The Ocean2k synthesis trends are insensitive to bin center placement (Supplementary Section 5; Supplementary Fig. S5). The mean of the distribution of the ages of individual data points within each bin is very close to the bin center (Supplementary Table S5). The 'binned' and standardized values are then treated as a sample of the SST population within each bin, with age uncertainty approximately equal to bin width. The numbers of chronological control points per bin are in Supplementary Figure S1. Slope and slope probabilities were estimated using Monte Carlo simulations (below). Our results are insensitive to standardization (Supplementary Section 4). All simulated SSTs were 'binned' and composited as described here.

Sensitivity tests were performed on the Ocean2k synthesis cooling trend to assess the influence of the following characteristics (Supplementary Table S1): *(i)* reconstruction type e.g. alkenone, foraminiferal Mg/Ca, other (microfossil transfer functions or modern analogue technique, TEX_{86} and coral Sr/Ca); *(ii)* response seasonality (mean-annual, warm, cool); *(iii)* number of ^{14}C dates/reconstruction (>4 or ≤4 ^{14}C dates; note – four reconstructions were not ^{14}C dated and are not included in this test (Supplementary Table S1)); *(iv)* sampling resolution (<8, ≥8 samples per bin); *(v)* sedimentation rate (≤0.1cm/yr, >0.1 cm/yr); *(vi)* water depth (>500 m, <500 m); *(vii)* basin (Arctic, Atlantic, Indian, Mediterranean, Pacific, Southern); *(viii)* latitude (extratropical Northern Hemisphere (NH) [>30°N], "tropical" [30°N-30°S], extratropical Southern Hemisphere (SH) [>30°S]); *(ix)* hemisphere (Northern or Southern); and *(x)* locations within pre-defined upwelling zones (Supplementary Table S3). The sub-datasets were binned, standardized and composited as per the Ocean2k synthesis. Medians are plotted in Figure 2b. We use water depth as a proxy for open ocean conditions (Supplementary Section 6). Maps of each sensitivity analysis (Supplementary Fig. S9) were generated to examine the potential spatial bias associated with each characteristic.

Each bin value (in each sensitivity test) represents a standardized mean of up to 57 data points per 200-yr bin, and the full 2000-yr dataset includes 10 standard deviations (one value per bin). Therefore, to represent the overall error for each sensitivity analysis, a median standard deviation of the 10 bins was calculated, and is plotted in the error histograms (Fig. 2b, right).

Slopes and slope probabilities were estimated from Monte Carlo simulations. 10,000 linear least-squares fits were estimated; for each realization a single observation from each bin of a given synthesis was randomly selected (with replacement) to create the fit estimate. The median slope of these fits was then calculated. Slopes were similarly estimated for the Ocean2k synthesis (Fig. 2-4), Terrestrial 2k and multi-model composite (Fig. 3), and single and cumulative forcing model SST estimates (Fig. 4; Supplementary Fig. S11). Slopes in Figure 4 are plotted with +/–2 standard errors of the mean, assuming a normally distributed sample of the regression slope.

Data availability Data URLs for the 57 reconstructions are in Supplementary Table S2. Ocean2k SST synthesis data matrix are here: http://www.ncdc.noaa.gov/paleo/study/18718. Model output URLs are in Supplementary Table S4. Terrestrial 2k composite data are here: https://www.ncdc.noaa.gov/cdo/f?p=519:2:0::::P1_study_id:12621 and update 1.1.1 http://dx.doi.org/10.6084/m9.figshare.1054736

Code availability. The compositing code used to generate the Ocean2k SST synthesis (Fig. 2a) is here: http://www.ncdc.noaa.gov/paleo/study/18718.

Supplementary Information is linked to the online version of the paper at XXXXX.

References

1 Moberg, A., Sonechkin, D. M., Holmgren, K., Datsenko, N. M. & Karlen, W. Highly variable Northern Hemisphere temperatures reconstructed from low- and high-resolution proxy data. *Nature* **433**, 613-617, 10.1038/nature03265 (2005).

2 Mann, M. E., Zhang, Z., Rutherford, S., Bradley, R. S., Hughes, M. K., Shindell, D., Ammann, C., Faluvegi, G. & Ni, F. Global Signatures and Dynamical Origins of the Little Ice Age and Medieval Climate Anomaly. *Science* **326**, 1256-1260, 10.1126/science.1177303 (2009).

3 Jones, P. D. *et al.* High-resolution palaeoclimatology of the last millennium: a review of current status and future prospects. *The Holocene* **19**, 3-49, 10.1177/0959683608098952 (2009).

4 Braconnot, P., Harrison, S. P., Kageyama, M., Bartlein, P. J., Masson-Delmotte, V., Abe-Ouchi, A., Otto-Bliesner, B. & Zhao, Y. Evaluation of climate models using palaeoclimatic data. *Nature Climate Change* **2**, 417-424, 10.1038/nclimate1456 (2012).

5 Marcott, S. A., Shakun, J. D., Clark, P. U. & Mix, A. C. A Reconstruction of Regional and Global Temperature for the Past 11,300 Years. *Science* **339**, 1198-1201, 10.1126/science.1228026 (2013).

6 Schmidt, G. A., Jungclaus, J. H., Ammann, C. M., Bard, E., Braconnot, P., Crowley, T. J., Delaygue, G., Joos, F., Krivova, N. A., Muscheler, R., Otto-Bliesner, B. L., Pongratz, J., Shindell, D. T., Solanki, S. K., Steinhilber, F. & Vieira, L. E. A. Climate forcing reconstructions for use in PMIP simulations of the Last Millennium (v1.1). *Geoscientific Model Development* **5**, 185-191, 10.5194/gmd-5-185-2012 (2012).

7 PAGES 2k Consortium. Continental-scale temperature variability during the past two millennia. *Nature Geoscience* **6**, 339-346, 10.1038/ngeo1797 (2013).

8 Gill, A. E. in *Atmosphere–Ocean Dynamics* **Vol. 30** *International Geophysics Series* (Academic Press, London, 1982).

9 Balmaseda, M. A., Trenberth, K. E. & Källén, E. Distinctive climate signals in reanalysis of global ocean heat content. *Geophysical Research Letters* **40**, 1754-1759, 10.1002/grl.50382 (2013).

10 Rhein, M., Rintoul, S. R., Aoki, S., Campos, E., Chambers, D., Feely, R. A., Gulev, S., Johnson, G. C., Josey, S. A., Kostianoy, A., Mauritzen, C., Roemmich, D., Talley, L. D. & Wang, F. in *Climate Change 2013: The Physical Science Basis. Contribution of Working Group I to the Fifth Assessment Report of the Intergovernmental Panel on Climate Change* (eds T.F. Stocker *et al.*) (Cambridge University Press, Cambridge, United Kingdom and New York, NY, USA, 2013).

11 Kennedy, J. J. A review of uncertainty in in situ measurements and data sets of sea surface temperature. *Reviews of Geophysics* **52**, 1-32, 10.1002/2013rg000434 (2014).

12 Lee, T. C. K., Zwiers, F. W. & Tsao, M. Evaluation of proxy-based millennial reconstruction methods. *Climate Dynamics* **31**, 263-281, 10.1007/s00382-007-0351-9 (2008).

13 Mann, M. E., Zhang, Z. H., Hughes, M. K., Bradley, R. S., Miller, S. K., Rutherford, S. & Ni, F. B. Proxy-Based Reconstructions of Hemispheric and Global Surface Temperature Variations over the Past Two Millennia. *Proceedings of the National Academy of Sciences* **105**, 13252-13257, 10.1073pnas.0805721105 (2008).

14 Evans, M. N., Tolwinski-Ward, S. E., Thompson, D. M. & Anchukaitis, K. J. Applications of proxy system modeling in high resolution paleoclimatology. *Quaternary Science Reviews* **76**, 16-28, 10.1016/j.quascirev.2013.05.024 (2013).

15 Lohmann, G., Pfeiffer, M., Laepple, T., Leduc, G. & Kim, J. H. A model–data comparison of the Holocene global sea surface temperature evolution. *Climate of the Past* **9**, 1807-1839, 10.5194/cp-9-1807-2013 (2013).

16 Laepple, T. & Huybers, P. Global and regional variability in marine surface temperatures. *Geophysical Research Letters* **41**, 2528-2534, 10.1002/2014GL059345 (2014).

17 Lamb, H. H. The early medieval warm epoch and its sequel. *Palaeogeography, Palaeoclimatology, Palaeoecology* **1**, 13-37, 10.1016/0031-0182(65)90004-0 (1965).

18 Neukom, R., Gergis, J., Karoly, D. J., Wanner, H., Curran, M., Elbert, J., Gonzalez-Rouco, F., Linsley, B. K., Moy, A. D., Mundo, I., Raible, C. C., Steig, E. J., van Ommen, T., Vance, T., Villalba, R., Zinke, J. & Frank, D. Inter-hemispheric temperature variability over the past millennium. *Nature Climate Change* **4**, 362-367, 10.1038/nclimate2174 (2014).

19 Kaplan, A., Cane, M. A., Kushnir, Y., Clement, A. C., Blumenthal, M. B. & Rajagopalan, B. Analyses of global sea surface temperature 1856–1991. *Journal of Geophysical Research-Oceans* **103**, 18567-18589, 10.1029/97jc01736 (1998).

20 Allan, R., Brohan, P., Compo, G. P., Stone, R., Luterbacher, J. & Bronniman, S. The International Atmospheric Circulation Reconstructions over the Earth (ACRE) Initiative. *Bulletin of the American Meteorological Society* **92**, 1421-1425, 10.1175/2011BAMS3218.1 (2011).

21 Emile-Geay, J., Cobb, K. M., Mann, M. E. & Wittenberg, A. T. Estimating Central Equatorial Pacific SST Variability over the Past Millennium. Part I: Methodology and Validation. *Journal of Climate* **26**, 2302–2328, 10.1175/JCLI-D-11-00510.1 (2013).

22 Tierney, J. E., Abram, N. J., Anchukaitis, K. J., Evans, M. N., Giry, C., Kilbourne, K. H., Saenger, C. P., Wu, H. C. & Zinke, J. Tropical sea-surface temperatures for the

past four centuries reconstructed from coral archives. *Paleoceanography*, 10.1002/2014PA002717 (2015).

23 Evans, M. N., Kaplan, A. & Cane, M. A. Pacific sea surface temperature field reconstruction from coral $\delta^{18}O$ data using reduced space objective analysis. *Paleoceanography* **17**, 10.1029/2000PA000590 (2002).

24 Masson-Delmotte, V., Schulz, M., Abe-Ouchi, A., Beer, J., Ganopolski, A., González Rouco, J. F., Jansen, E., Lambeck, K., Luterbacher, J., Naish, T., Osborn, T., Otto-Bliesner, B., Quinn, T., Ramesh, R., Rojas, M., Shao, X. & Timmermann, A. in *Climate Change 2013: The Physical Science Basis. Contribution of Working Group I to the Fifth Assessment Report of the Intergovernmental Panel on Climate Change* (eds T.F. Stocker *et al.*) (Cambridge University Press, Cambridge, United Kingdom and New York, NY, USA, 2013).

25 McKay, N. P. & Kaufman, D. S. An extended Arctic proxy temperature database for the past 2,000 years. *Scientific Data* **1**, 10.1038/sdata.2014.26 (2014).

26 Phipps, S. J., McGregor, H. V., Gergis, J., Gallant, A. J. E., Neukom, R., Stevenson, S., Ackerley, D., Brown, J. R., Fischer, M. J. & van Ommen, T. D. Paleoclimate Data–Model Comparison and the Role of Climate Forcings over the Past 1500 Years. *Journal of Climate* **26**, 6915-6936, 10.1175/jcli-d-12-00108.1 (2013).

27 Crespin, E., Goosse, H., Fichefet, T., Mairesse, A. & Sallaz-Damaz, Y. Arctic climate over the past millennium: Annual and seasonal responses to external forcings. *The Holocene* **23**, 321-329, 10.1177/0959683612463095 (2013).

28 Delaygue, G. & Bard, E. An Antarctic view of Beryllium-10 and solar activity for the past millennium. *Climate Dynamics* **36**, 2201-2218, 10.1007/s00382-010-0795-1 (2011).

29 Schurer, A. P., Tett, S. F. B. & Hegerl, G. C. Small influence of solar variability on climate over the past millennium. *Nature Geoscience* **7**, 104-108, 10.1038/ngeo2040 (2014).

30 Bard, E. & Frank, M. Climate change and solar variability: What's new under the sun? *Earth and Planetary Science Letters* **248**, 1-14, 10.1016/j.epsl.2006.06.016 (2006).

31 Rind, D., Lean, J., Lerner, J., Lonergan, P. & Leboissitier, A. Exploring the stratospheric/tropospheric response to solar forcing. *Journal of Geophysical Research: Atmospheres* **113**, D24103, 10.1029/2008JD010114 (2008).

32 Berger, A. L. Long-Term Variations of Daily Insolation and Quaternary Climatic Changes. *Journal of the Atmospheric Sciences* **35**, 2362-2367, 10.1175/1520-0469(1978)035<2362:LTVODI>2.0.CO;2 (1978).

33 Hays, J. D., Imbrie, J. & Shackleton, N. J. Variations in the Earth's Orbit: Pacemaker of the Ice Ages. *Science* **194**, 1121-1132, 10.1126/science.194.4270.1121 (1976).

34 Esper, J., Frank, D. C., Timonen, M., Zorita, E., Wilson, R. J. S., Luterbacher, J., Holzkamper, S., Fischer, N., Wagner, S., Nievergelt, D., Verstege, A. & Buntgen, U. Orbital forcing of tree-ring data. *Nature Climate Change* **2**, 862-866, 10.1038/nclimate1589 (2012).

35 Kaufman, D. S., Schneider, D. P., McKay, N. P., Ammann, C. M., Bradley, R. S., Briffa, K. R., Miller, G. H., Otto-Bliesner, B. L., Overpeck, J. T., Vinther, B. M. & Members, A. L. k. P. Recent Warming Reverses Long-Term Arctic Cooling. *Science* **325**, 1236-1239, 10.1126/science.1173983 (2009).

36 Brovkin, V., Claussen, M., Driesschaert, E., Fichefet, T., Kicklighter, D., Loutre, M., Matthews, H., Ramankutty, N., Schaeffer, M. & Sokolov, A. Biogeophysical effects of historical land cover changes simulated by six Earth system models of intermediate complexity. *Climate Dynamics* **26**, 587-600, 10.1007/s00382-005-0092-6 (2006).

37 Goosse, H., Arzel, O., Luterbacher, J., Mann, M. E., Renssen, H., Riedwyl, N., Timmermann, A., Xoplaki, E. & Wanner, H. The origin of the European "Medieval Warm Period". *Climate of the Past* **2**, 99-113, 10.5194/cp-2-99-2006 (2006).

38 de Noblet-Ducoudré, N., Boisier, J.-P., Pitman, A., Bonan, G. B., Brovkin, V., Cruz, F., Delire, C., Gayler, V., van den Hurk, B. J. J. M., Lawrence, P. J., van der Molen, M. K., Müller, C., Reick, C. H., Strengers, B. J. & Voldoire, A. Determining Robust Impacts of Land-Use-Induced Land Cover Changes on Surface Climate over North America and Eurasia: Results from the First Set of LUCID Experiments. *Journal of Climate* **25**, 3261-3281, 10.1175/jcli-d-11-00338.1 (2012).

39 He, F., Vavrus, S. J., Kutzbach, J. E., Ruddiman, W. F., Kaplan, J. O. & Krumhardt, K. M. Simulating global and local surface temperature changes due to Holocene anthropogenic land cover change. *Geophysical Research Letters* **41**, 623–631, 10.1002/2013GL058085 (2014).

40 Hansen, J., Lacis, A., Ruedy, R. & Sato, M. Potential climate impact of Mount Pinatubo eruption. *Geophysical Research Letters* **19**, 215-218, 10.1029/91GL02788 (1992).

41 Robock, A. Volcanic eruptions and climate. *Reviews of Geophysics* **38**, 191-219, 10.1029/1998RG000054 (2000).

42 Stenchikov, G., Delworth, T. L., Ramaswamy, V., Stouffer, R. J., Wittenberg, A. & Zeng, F. Volcanic signals in oceans. *Journal of Geophysical Research-Atmospheres* **114**, D16104, 10.1029/2008JD011673 (2009).

43 Miller, G. H., Geirsdóttir, Á., Zhong, Y., Larsen, D. J., Otto-Bliesner, B. L., Holland, M. M., Bailey, D. A., Refsnider, K. A., Lehman, S. J., Southon, J. R., Anderson, C., Björnsson, H. & Thordarson, T. Abrupt onset of the Little Ice Age triggered by

volcanism and sustained by sea-ice/ocean feedbacks. *Geophysical Research Letters* **39**, L02708, 10.1029/2011gl050168 (2012).

44 Plummer, C. T., Curran, M. A. J., van Ommen, T. D., Rasmussen, S. O., Moy, A. D., Vance, T. R., Clausen, H. B., Vinther, B. M. & Mayewski, P. A. An independently dated 2000-yr volcanic record from Law Dome, East Antarctica, including a new perspective on the dating of the 1450s CE eruption of Kuwae, Vanuatu. *Climate of the Past* **8**, 1929-1940, 10.5194/cp-8-1929-2012 (2012).

45 Sigl, M., McConnell, J. R., Toohey, M., Curran, M., Das, S. B., Edwards, R., Isaksson, E., Kawamura, K., Kipfstuhl, S., Kruger, K., Layman, L., Maselli, O. J., Motizuki, Y., Motoyama, H., Pasteris, D. R. & Severi, M. Insights from Antarctica on volcanic forcing during the Common Era. *Nature Climate Change* **4**, 693-697, 10.1038/nclimate2293 (2014).

46 Goosse, H., Barriat, P. Y., Lefebvre, W., Loutre, M. F. & Zunz, V. *Introduction to climate dynamics and climate modeling. Online textbook available at* http://www.climate.be/textbook, 2015).

47 Crowley, T. J. Causes of Climate Change Over the Past 1000 Years. *Science* **289**, 270-277, 10.1126/science.289.5477.270 (2000).

48 Zhong, Y., Miller, G. H., Otto-Bliesner, B. L., Holland, M. M., Bailey, D. A., Schneider, D. P. & Geirsdottir, A. Centennial-scale climate change from decadally-paced explosive volcanism: a coupled sea ice-ocean mechanism. *Climate Dynamics* **37**, 2373-2387, 10.1007/s00382-010-0967-z (2011).

49 Mignot, J., Khodri, M., Frankignoul, C. & Servonnat, J. Volcanic impact on the Atlantic Ocean over the last millennium. *Climate of the Past* **7**, 1439-1455, 10.5194/cp-7-1439-2011 (2011).

50 Ding, Y., Carton, J. A., Chepurin, G. A., Stenchikov, G., Robock, A., Sentman, L. T. & Krasting, J. P. Ocean response to volcanic eruptions in Coupled Model Intercomparison Project 5 simulations. *Journal of Geophysical Research: Oceans* **119**, 5622-5637, 10.1002/2013JC009780 (2014).

Correspondence and requests for materials should be addressed to Helen V. McGregor.

Acknowledgements

We thank the many scientists who made their published datasets available via public data repositories. T. Kiefer, L. von Gunten and C. Telepski from the IGBP PAGES-IPO provided organizational and logistical support. V. Masson-Delmotte, C. Giry, S.P. Bryan, S. Stevenson, D. Colombaroli, B. Horton, J. Tierney and the Ocean2k HR Working Group are thanked for early input to the project design and methodology. G. Lohmann assisted with model output. A. Mairesse assisted with model figures. L. Skinner and D. Reynolds are thanked for discussions on age models. We are grateful to the 75 volunteers who constructed the Ocean2k metadatabase (see Supplement Information for full list of names). We acknowledge support from PAGES, a core project of IGBP funded by the US and Swiss National Science Foundations (NSF) and NOAA; Australian Research Council (ARC) *Discovery Project* grant DP1092945 (H.V.M., S.J.P.), ARC *Future Fellowship* FT140100286 grant (H.V.M.), AINSE Fellowship grant (H.V.M.), and the research contributes to ARC *Australian Laureate Fellowship* FL120100050; US NSF awards NSF/ATM09-02794 (M.N.E.) and NSF/ATM0902715 (M.N.E), and Royal Society of New Zealand Marsden Fund grant 11-UOA-027 (M.N.E.); F.R.S-FNRS (Belgium) (H.G.); French National Research Agency (ANR) under ISOBIOCLIM grant (G.L.); European Union's Seventh Framework programme

(FP7/2007-2013) under Grant agreement number 243908, 'Past4Future, Climate change—Learning from the past climate' contribution #81 (H.G., B.M., P.G.M., M.-S.S.); CSIC-Ramón y Cajal post-doctoral program RYC-2013-14073 (B.M.), Clare Hall College, Cambridge, Shackleton Fellowship (B.M.), and GRACCIE CSD2007-00067 Programa Consolider-Ingenio 2010 (B.M.); US Geological Survey's Climate and Land Use Change Research and Development Program and the Volcano Science Center (J.A.A.); Ralph E. Hall Endowed Award for Innovative Research (D.W.O.); Danish Council for Independent Research | Natural Science OCEANHEAT project 12-126709/FNU (M.-S.S.); LEFE/INSU/NAIV project (M.-A.S.); NSF of China grants 41273083 (K.S.), and Shanhai Fund grant 2013SH012 (K.S.); UTIG Ewing-Worzel Fellowship (K.T.); Swedish Research Council grant 621-2011-5090 (H.L.F.); and from a Marie Curie Intra-European Fellowship for Career Development (V.E.).

Author contributions

M.N.E., H.V.M., D.W.O., H.G., G.L. and B.M. designed the project with input from J.A.A., M.-S.S., M.-A.S., K.S. and V.E.; H.V.M. and G.L. led the synthesis. H.V.M. and B.M. collated and evaluated the reconstructions, and managed the data with assistance from J.A.A.; M.N.E. led the analysis with important contributions from H.G., J.A.A., B.M., G.L., S.J.P., H.V.M., D.W.O., P.G.M., M.-S.S. and M.-A.S.; H.G. and S.J.P. collated, managed, and analysed the model simulations with input from M.N.E., G.L. and H.V.M.; H.V.M. led the writing with the assistance of M.N.E., H.G., G.L., B.M., J.A.A., P.G.M., D.W.O., M.-S.S., M.-A.S., S.J.P., K.S., K.T., H.L.F, and V.E.; all authors reviewed the manuscript.

Competing financial interests

The authors declare no competing financial interests.

Figure Legends

Figure 1. Correlation map and locations of the 57 reconstructions in the Ocean2k SST synthesis. Map is based on six climate model simulations for the interval 801–1800 CE[4,6,26,27] (Supplementary Table S4). For each simulation, SST data were composited into 200-year 'bins', and the correlation between grid point SST and model global average SST calculated (Supplementary Section 5). The map shows the 6-model median correlation coefficient (colours). Numbers indicate where multiple SST reconstructions are from nearby locations. The correlation map qualitatively suggests that SST at the 57 locations is representative of global mean SST on centennial time scales.

Figure 2. Ocean2k global SST composite and sensitivity analyses. a. Standardized Ocean2k SST synthesis (lines are the N=57 reconstructions, coloured by ocean basin, see b)). Boxplots show 25th to 75th percentile range (black box), median (black line), and outliers (red crosses) to approximately 99.3% of data range (black dashed lines and cap) assuming bin contents are normally distributed (Methods). Black line is the median of the ocean basin area-weighted composite (Supplement section 5). **b.** Standardized 57 Ocean2k reconstructions resampled into a range of categories (medians plotted; Methods). Bar graphs give sensitivity-test error estimates, and number of reconstructions per subcategory (Methods).

Figure 3. Global SST and temperature trends for 801–1800 CE. a. Ocean2k SST synthesis (Fig. 2a). **b.** Terrestrial 2k composite (Supplementary Section 9). **c.** Multi-model composite, for the same locations and periods as reconstructions in a) (Methods; Supplementary Table S4). Boxplots show 25th to 75th percentile range (blue box), median (red line), and outliers (red crosses) to 99.3% of data range (blue 'whiskers') assuming bin contents are normally distributed (Supplementary Table S14). Distribution (grey lines) and

median (black line) of 10,000 Monte Carlo trend estimates are displayed for each synthesis. Trends are qualitatively similar between data and model composites.

Figure 4. 851–1850 CE Ocean2k SST synthesis and model simulation slopes, volcanic forcing, and EBM response. a. CSIRO Mk3L simulations (blue), and **b.** LOVECLIM simulations (yellow). Monte Carlo slopes (circles) and negative slope probabilities (bars; p=50%: equal probability of positive or negative slope; Methods). Ocean2k SST synthesis is also shown (O2k; red). Slope +/– 2 standard errors are smaller than the symbols. Time series in Supplementary Figure S11. **c.** Volcanic forcing, and **d.** EBM temperature response. 200-year bin averages (blue lines) and linear fit (straight line) are shown. Volcanic forcing contributes to the cooling trend via a thermodynamic response.

Figure 1

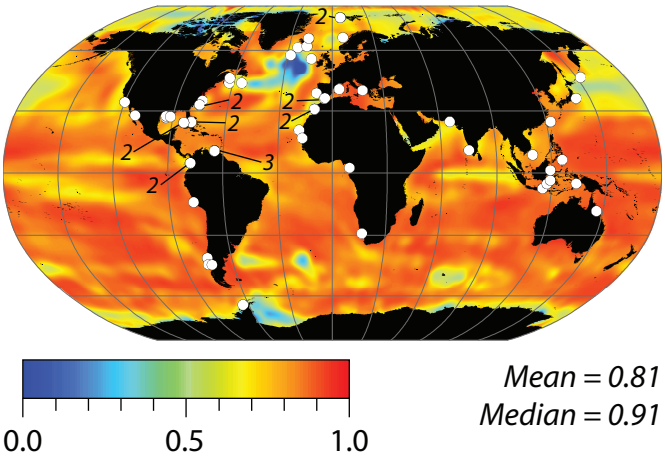

PMIP3 simulations:

bcc-csm1-1	CSIRO Mk3L_4	MPI-ESM
CCSM4	FGOALS-s2	LOVECLIM_PMIP3

Figure 2

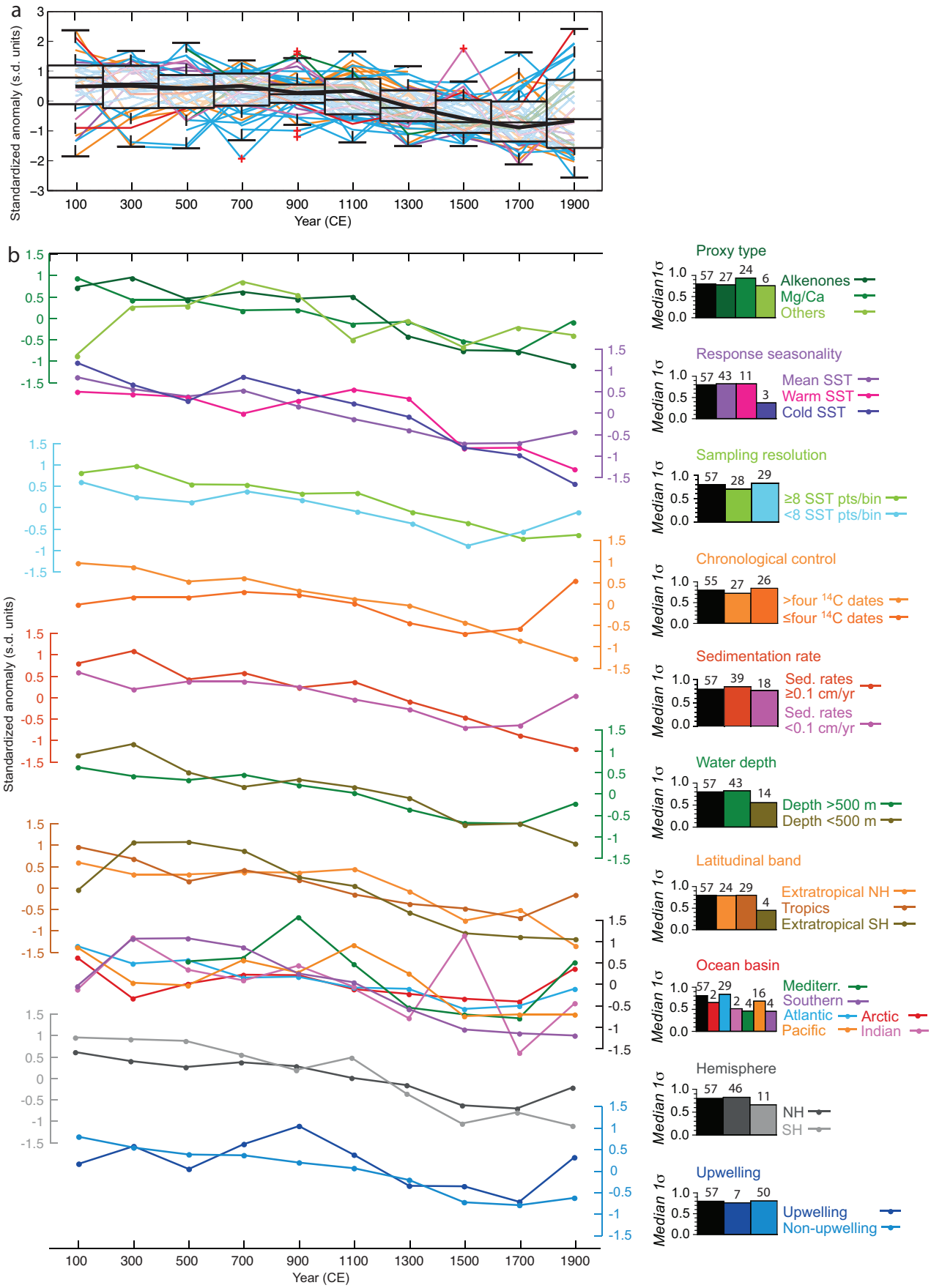
a
Standardized anomaly (s.d. units)
Year (CE)
b
Standardized anomaly (s.d. units)
Year (CE)
Proxy type
Alkenones
Mg/Ca
Others
Response seasonality
Mean SST
Warm SST
Cold SST
Sampling resolution
≥8 SST pts/bin
<8 SST pts/bin
Chronological control
>four 14C dates
≤four 14C dates
Sedimentation rate
Sed. rates ≥0.1 cm/yr
Sed. rates <0.1 cm/yr
Water depth
Depth >500 m
Depth <500 m
Latitudinal band
Extratropical NH
Tropics
Extratropical SH
Ocean basin
Mediterr.
Southern
Atlantic
Arctic
Pacific
Indian
Hemisphere
NH
SH
Upwelling
Upwelling
Non-upwelling
Median 1σ

Figure 3

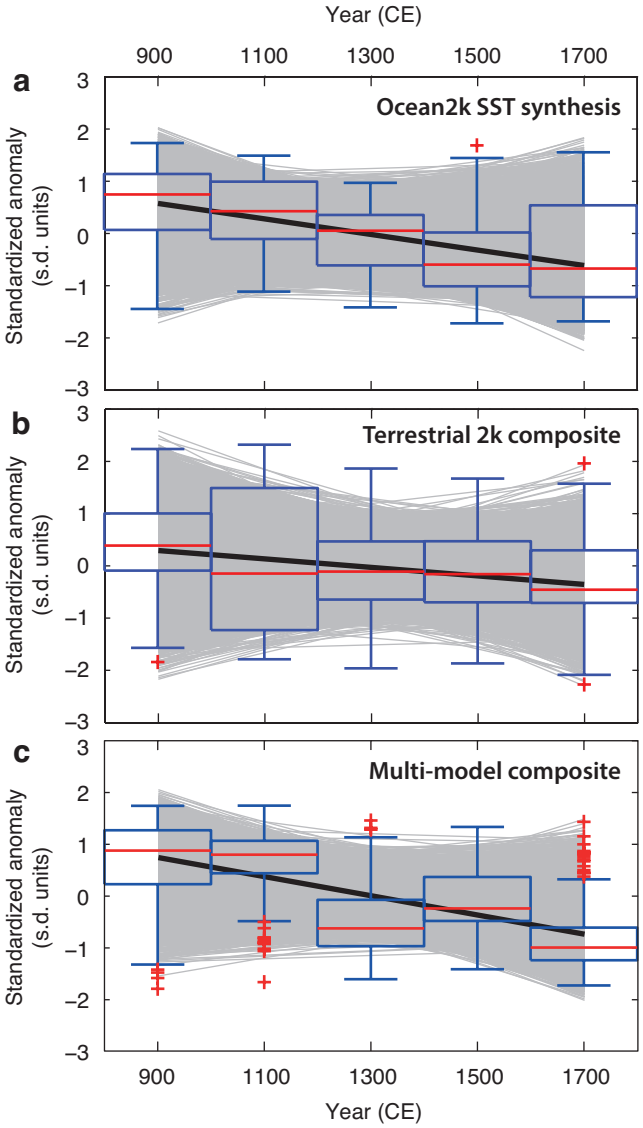
Year (CE)
900
1100
1300
1500
1700
a
Ocean2k SST synthesis
b
Terrestrial 2k composite
c
Multi-model composite
Standardized anomaly (s.d. units)
3
2
1
0
−1
−2
−3

Figure 4

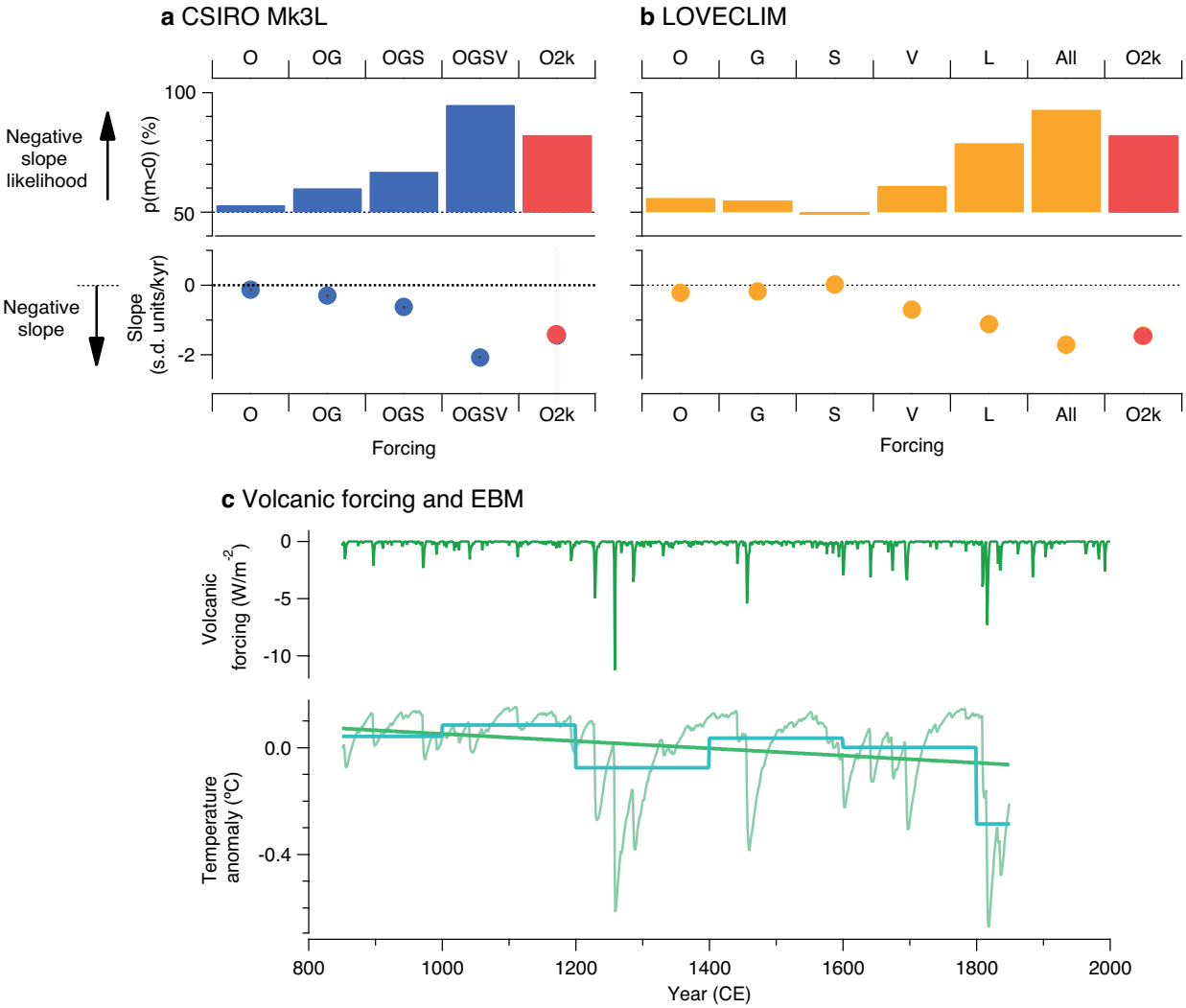
a CSIRO Mk3L
b LOVECLIM
O
OG
OGS
OGSV
O2k
G
S
V
L
All
Negative slope likelihood
p(m<0) (%)
100
50
Negative slope
Slope (s.d. units/kyr)
0
-2
Forcing
c Volcanic forcing and EBM
Volcanic forcing (W/m-2)
0
-5
-10
Temperature anomaly (°C)
0.0
-0.4
800
1000
1200
1400
1600
1800
2000
Year (CE)